Heat Transfer from Catalysts with Computational Fluid Dynamics

Timothy F. McKenna and Roger Spitz
CNRS-LCPP/CPE, 69616 Villeurbanne, France

Davor Cokljat
FLUENT Europe Ltd., Sheffield S11 9LP, U.K.

A computational fluid dynamics software package was used to study heat transfer from spherical particles of different sizes and under different heat-transfer conditions. It was shown that although the Ranz-Marshall and other similar correlations are valid in the case where particles do not interact, this is not true for densely packed systems such as those that we find in reactors commonly used in olefin polymerization. It was also demonstrated that convection is in fact not the only means of removing heat from small, highly active particles. Conductive heat transfer between large and small particles present in the same reactor appears to help alleviate problems of overheating and explain why earlier models of heat transfer in olefin polymerization overpredict the temperature rise during early stages of polymerization.

Introduction

Processes for the polymerization of olefins using ''low pressure processes'' (so-called because they run at 20 to 30 bar with respect to the 1,500–3,000 bar of the much older free-radical process) are in full growth. The development of highly active Ziegler-Natta, and more recently supported metallocene catalysts make such processes very attractive and offer one the possibility of producing tailor-made polymers in rather mild, and therefore less expensive, process conditions. Gas-phase processes are, in theory, particularly interesting because they use no solvents and because of the ease of separation of the final product from the reaction medium. However, the use of highly active heterogeneous catalysts has produced some very interesting chemical engineering phenomena, particularly in the area of heat and mass transfer. It is a well accepted (and rather obvious) fact that an understanding of the mechanisms underlying heat and mass transfer in reacting systems is a *sine qua non* for proper reactor design, optimization, and control. It is for this reason that numerous university research groups and companies have invested so much time and energy is trying to model these coupled phenomena in the particular case of heterogeneously catalyzed olefin polymerizations, and in particular the polymerization of ethylene and of propylene in gas-phase reactors (such as Xie et al., 1994; Taylor et al., 1981; Soares and Hamielec, 1995; McKenna et al., 1995a,b, 1997a,b, 1998, 1999; Laurence and Chiovetta, 1983; Hutchinson et al., 1991, 1992; Floyd et al., 1986a,b,c, 1987; Ferrero and Chiovetta, 1987a,b, 1997a,b).

To put the problem of particle heat and mass transfer into perspective, consider the different length scales involved in the process shown in Figure 1. While this figure focuses on a gas-phase fluidized-bed reactor (FBR), the different length scales and transfer phenomena are the same in liquid phase (slurry or liquid pool) processes. As one can easily imagine, the detailed modeling of such a reactor is a highly complex task involving reactor design, complex multiphase flows, interphase mass transfer, particle–particle and particle–reactor interactions, intraparticle heat and mass transfer, and nanoscale phenomena such as the chemistry and kinetics of the active sites of the catalyst and the crystallization of the polymer. We will only consider the problem of heat transfer in a gas-phase process at the level of one, two, or three neighboring particles in the current work, which correspond to length scales on the order of tens to hundreds of microns.

The reaction and evolution of morphology in the heterogeneously supported particles are complex, and very rapid. At the risk of oversimplifying the particle growth process shown

Correspondence concerning this article should be addressed to T. F. McKenna.

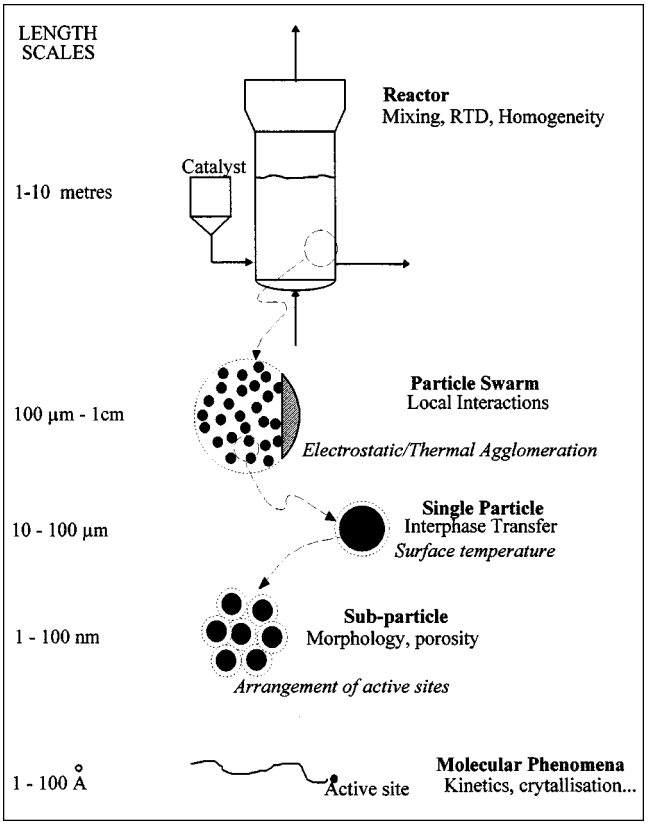

Figure 1. Phenomena and length scales involved in polyolefin processes.

in Figure 2, it can be described using either the multigrain model (MGM), or, with some additional simplifications, the polymeric flow model (PFM) (see, for example, Laurence and Chiovetta, 1983). The original catalyst particle used in the polymerization is composed of a solid, porous support. Active sites, the place where the polymerization actually occurs, are activated metallic complexes that are distributed on the surface of the elementary particles inside the pores of the support. Catalysts currently used in this type of process can be divided into three main groups: metallocenes, Phillips, and Ziegler-Natta (ZN) catalysts. The difference between these two types of catalysts lies almost exclusively in their chemical preparation, and the way in which the polymer chains are formed at the active sites. However, when the catalysts are supported, the basic physical processes of transfer are the same in both cases, and any heat- and mass-transfer resistance that might or might not occur are to a very large extent independent of the catalyst system in use.

Initially, the monomer must diffuse from the continuous external phase, through the boundary layer around the particle, and through the pores to the active sites where it forms a solid polymer. The active sites are covered almost immediately with a layer of polymer that adds a further barrier through which the monomer must diffuse in order for the reaction to take place. After the first few seconds at most, the hydraulic forces created by the formation of solid polymer inside the particle cause the original structure to rupture, or fragment. The particle retains its original shape because of the entanglement and/or crystallization of the macromolecules formed in the porous structure of the originally porous support. Thus what was once a catalyst particle becomes a ''polymer particle'' composed of a continuous, porous polymer phase in which fragments of the original catalyst particle are suspended. This rupture of the continuous catalyst particles allows the reaction to continue at a very rapid rate—on the order of several tonnes of polymer per gram of catalyst per hour—and thus to grow rapidly from an originally very small particle (10 μm) to a final size on the order of 1 mm. It should be noted that since the reaction is very fast, with typical rates on the order of 30,000 to 60,000 g of polymer per gram of catalyst per hour (g/g/h), the transformation of particle morphology and particle growth are also very fast, especially in the early stages. The particle fragmentation process is thought to take on the order of a few seconds (Ferrero and Chiovetta, 1987a,b). This process can take place in a gas phase, a liquid phase (slurry or suspension), or a three phase system (gas/liquid/solid).

Given that the polymerization of olefins is a highly exothermic reaction, with heats of polymerization on the order of 100–110 kJ/mol, heat production rates are extremely high inside a polymerization particle. Large temperature excursions in and around growing particles can be very dangerous because the reaction is typically carried out at a temperature of 80–90°C, and the melting point of the polymer will vary from 105°C to 135°C depending on its composition. From the point of view of understanding, mastering, and optimizing a chemical process, how we go about modeling the heat-transfer problem is therefore of a great importance. The research groups of Chiovetta at the University of Buenos Aires, and of Ray at the University of Wisconsin (Madison) were the first to do an in-depth investigation of heat-transfer phe-

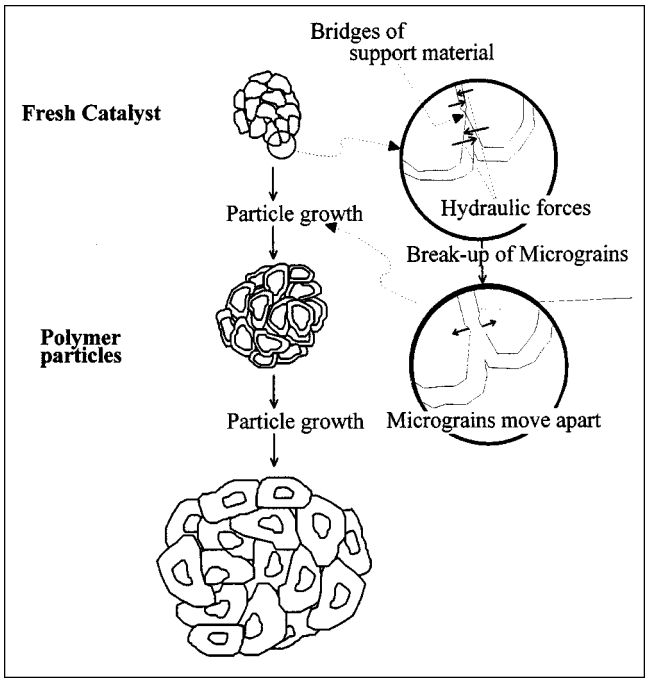

Figure 2. Transformation of a fresh catalyst particle into a polymer particle, and evolution of particle morphology and growth.

nomena in and around fresh catalyst, and growing polymer particles. They pointed out in a number of articles that heat-transfer problems can be important in gas-phase reactions (such as Floyd et al., 1986a,b,c, 1987), but probably not so much in slurry or liquid-phase reactions. As one would suspect, heat-transfer problems (that is, large temperature rises in and around the particles) are most important on fresh particles (no polymerization) with high activities. Also, the larger the initial particle size, the greater the potential for heat-transfer difficulties. This is not surprising since the rate of heat generation will be proportional to the number of active sites per unit volume, whereas heat removal, be it by convection or conduction, is at best proportional to the surface area. Heat generation to removal rates are thus inversely proportional to the particle radius. As a result, if the particles "survive" to grow to much more than 2 or 3 times their original size, it is unlikely that the evacuation of energy from them becomes a difficult task. In fact this is doubly true since a large number of highly active catalysts deactivate as the reaction progresses.

In the case of ZN catalysts, most modeling work (see references previously cited) of temperature profiles inside the growing particles was predicted using an equation of the form

$$\frac{\partial T}{\partial t} = \nabla\cdot(k_e \nabla T) + \sum \Delta H_p R_p. \tag{1a}$$

For a spherical catalyst particle, in initial and boundary conditions are typically

$$T = T^0 \qquad \text{for } t = 0$$

$$\frac{\partial T}{\partial r} = 0 \qquad \text{for } r = 0 \tag{1b}$$

$$\text{(symmetry at particle center)} \tag{1c}$$

$$-\frac{\partial T}{\partial r} = \frac{h}{\rho C_p}(T_{\text{Bulk}} - T_{\text{surface}}) \qquad \text{for } r = R \tag{1d}$$

$$[\text{surface, with } R = R(t)].$$

This energy balance is coupled to a mass balance via the rate of reaction, R_p:

$$R_p = k_p C^*[M]. \tag{2}$$

In this admittedly simplified expression, $k_p C^*$ is an empirical rate constant that is a function of temperature, time, and a number of process variables; and $[M]$ is the concentration of monomer at the active sites. The expression $k_p C^*$ is a function of temperature, reaction rate, and radial position within the particle.

Further simplifying assumptions (aside from sphericity) include the fact that the particle is said to be a pseudohomogeneous medium (implying that the characteristic length scale for heat and mass transfer is the particle radius). Also it is supposed that there is no convection of any kind inside the particle. Finally, it is implicitly assumed in boundary condition (Eq. 1d) that heat transfer between the particle and the bulk of the reactor takes place via convection only, and is controlled by the film-side convective heat-transfer coefficient 'h'. This is one of the key heat-transfer parameters, and has been the focus of much attention in work on gas–solid reactions. The majority of works on olefin polymerization published until now have relied on the use of "traditional" chemical engineering correlations (such as Ranz and Marshall, 1952) based on an estimate of the Nusselt number (Nu) to predict heat- and mass-transfer coefficients around the growing polymer particles. It has been pointed out (such as McKenna et al., 1995a,b, 1999) that these existing descriptions of heat transfer are inadequate for modern, highly active catalytic systems for a number of reasons. Three of the most important follow:

1. The fact that existing correlations for the estimation of heat-transfer coefficients are based on work with particles of a few hundred microns or more (initial particle sizes in olefin processes are on the order of 10 to 20 microns in diameter)
2. These models assume that heat removal from growing particles is accomplished purely via a convective mechanism
3. The models used to predict how heat is evacuated from polymerizing systems do not account for the interaction of the particles with their immediate environment.

If one considers only the relatively low rates of reaction (activities), and thus relatively low rates of heat emission from the particles simulated in the earlier works cited above (about 1/10th to 1/50th of the activities currently obtained in industrial and laboratory reactors), it was perhaps not unreasonable to use such correlations and to make implicit assumptions on the mechanism of heat removal from the particles. Nevertheless, as we will see below, it is not realistic to attempt to model modern catalytic systems supposing that all heat is removed via convection, and there is no interaction between the particle and its environment. It has previously been argued that using ill-adapted heat-transfer coefficients would lead to predictions of overheating at the center of the catalyst particles, which in turn would cause the polymer to melt, fill the pores of the growing particle, and thus cause the reaction to slow down or stop completely due to severe mass-transfer resistance. In such an event, one would never encounter bed meltdown—an event that is all too common. For this reason, we have begun to search for a better description of the phenomena that govern heat transfer in gas-phase polyolefin reactors.

This is not to say that nobody has attempted to develop methods that incorporate particle–particle interactions into estimates of the heat-transfer coefficient; however, most of the previous work has been done using nonpolymerizing systems. For instance, Rowe and Claxton (1965), and Brodkey et al. (1994) take particle–particle or particle–wall interactions into account and provide expressions that calculate higher values of Nu (and thus h) than does the Ranz-Marshall correlation. In fact, Brodkey's expression yields values 20 to 100 times greater than those found for an isolated sphere. The latter authors claim that the presence of other particles facilitates heat transfer because of collisions that pierce the particle boundary layer.

Martin (1979, 1984) also considered particle–wall interactions, and claimed that this type of heat transfer can become dominant for particles smaller than one millimeter in gas fluidized beds. He also provides a correlation for porous beds that predicts heat-transfer coefficient values 2 to 3 times greater than those found for single particles. This increase in

heat-transfer rates is explained by variations in the superficial velocity of the gas phase of the reactor due to variations in the porosity of the bed. This type of contact would certainly facilitate heat transfer in general, especially if there were repeated and/or prolonged contact between hot particles and a cooler structure, for instance, the reactor wall or a larger less reactive particle. This in turn would help to explain—at least in part—why we remove more heat from the particles than is predicted by single-sphere correlations.

Because of the length and time scales involved, as well as the physical difficulty of measuring heat-transfer coefficients on such rapidly evolving particles, it is very difficult to physically determine the mechanisms by which heat transfer actually occurs in this type of system. For this reason it was decided to use computation fluid dynamics (CFD) to probe the mechanisms by which heat can be evacuated. The current article therefore uses powerful CFD techniques to investigate how heat transfer occurs in this type of system; what influence flow conditions, particle size, and particle–particle interactions might have; and what the characteristic times for heat transfer are. By doing so, it is demonstrated that conduction rather than convection is one of the more dominant means of heat removal in polymerizing systems, and why some of the early models of heat transfer cited earlier overpredict the temperature rise inside small, highly active particles. Attention is focused on the polymerization of ethylene in conditions similar to those found in gas-phase fluidized bed reactors, but this should not be viewed as the only area to which the conclusions and methods can be applied. The mechanisms for heat transfer explored here are also valid for nonpolymerizing systems. Furthermore, we examine very simplified situations, and although these are chosen to be representative of the heat-transfer conditions in a real reactor, it should not be assumed that the simulations in what follows are intended to precisely model particle and/or reactor behavior under real polymerization conditions.

CFD Modeling and Simulations

Since it is very difficult to directly observe and model all of the phenomena involved, we decided to simulate particle behavior in a number of idealized settings. We have looked at this problem with FLUENT (Fluent Users Guide, 1998), a CFD code, that is used to calculate the velocity and temperature profiles at the particle surface, as well as the value of various dimensionless groups such as the *Nu* and the Peclet number (*Pe*) related to the heat transfer around both single- and multiple-particle configurations.

The following momentum and energy-balance equations were solved in two, spatial dimensions (x_1 and x_2) for around one, two, or three particles:

$$\frac{\partial}{\partial t}(\rho c_{p,g} T_g) + \frac{\partial}{\partial x_j}(\rho u_j c_{p,g} T_g) = \frac{\partial}{\partial x_j}\left[k_{e,g}\left(\frac{\partial T_g}{\partial x_j}\right)\right] \quad (3)$$

$$\frac{\partial}{\partial t}(\rho u_i) + \frac{\partial}{\partial x_j}(\rho \mu_j \mu_i) = -\frac{\partial p}{\partial x_i} + \frac{\partial}{\partial x_j}\left[\mu\left(\frac{\partial u_i}{\partial x_j} + \frac{\partial u_j}{\partial x_i}\right)\right]. \quad (4)$$

Table 1. Parameter Values and Particle Configurations

Parameter	Value
Particle size	20–500 (μm)
Particle configurations	1 single particle (free stream) 2 particles (in free stream): Touching, 1 diameter apart 2 diameters apart 3 particles: 2 large, 1 small
Relative velocities	0.02, 0.2, 0.75 m/s
Gas-phase density	40 kg/m^3
Gas-phase viscosity	1.1×10^{-5} kg/m/s
Gas-phase thermal conductivity	0.0214 W/m/K
Inlet gas temperature	350 K

In order to solve these equations, we used an unstructured control-volume technique whereby the domain is subdivided into discrete control volumes and the integration of equations is performed on the individual control volumes (Mathur and Murthy, 1997). Velocities, pressure, and temperature are all stored at the center of each control volume (collocated approach) and the pressure is coupled with velocity field through a simple algorithm. A second-order accurate discretization scheme is used for all simulations presented in this article, and full details about the scheme are available in Mathur and Murthy (1997).

Equations 3 and 4 were solved using a variety of conditions and the fluid properties defined in Table 1 in order to calculate the value of *Nu*, along with temperature fields and flow fields needed to study the heat-transfer mechanism. The conditions for which the equations were solved varied from relatively simple, constant surface-temperature problems, through constant heat-flux conditions, to the solution of problems with conducting bodies and constant volumetric rates of heat production. The simpler calculations were used in order to identify those problems that merited further study.

As in most instances where numerical calculations are involved, it is important to establish that the results are independent of the grid used in the simulations. This was done by establishing an initial grid, performing a series of calculations, refining the grid such that the control volumes near the particle were refined by a factor of 2 in each direction, and performing the same calculations. A typical example of the grid independence test performed in this study is shown in Figure 3, where it can be seen that quite rigorous grid refinement from grid 1 (Figure 3a) to grid 2 (Figure 3b) does not influence *Nu* at the particle surface (Figure 3c). The difference between the coarse and refined grids is less than 4% at most. Furthermore, we can see from Figure 3c that additional grid refinement (grid not shown) leads to no changes in the calculated values for this example. Similar calculations were performed for the different simulations discussed in this article, although the results of such calculations are not shown for reasons of space. We can therefore be confident that the results presented throughout this article are grid-independent.

It should be noted that most of the simulations that follow are done under steady-state conditions. It will be shown in a later section that this assumption is valid, and that it does not change the final conclusions (qualitatively or quantitatively).

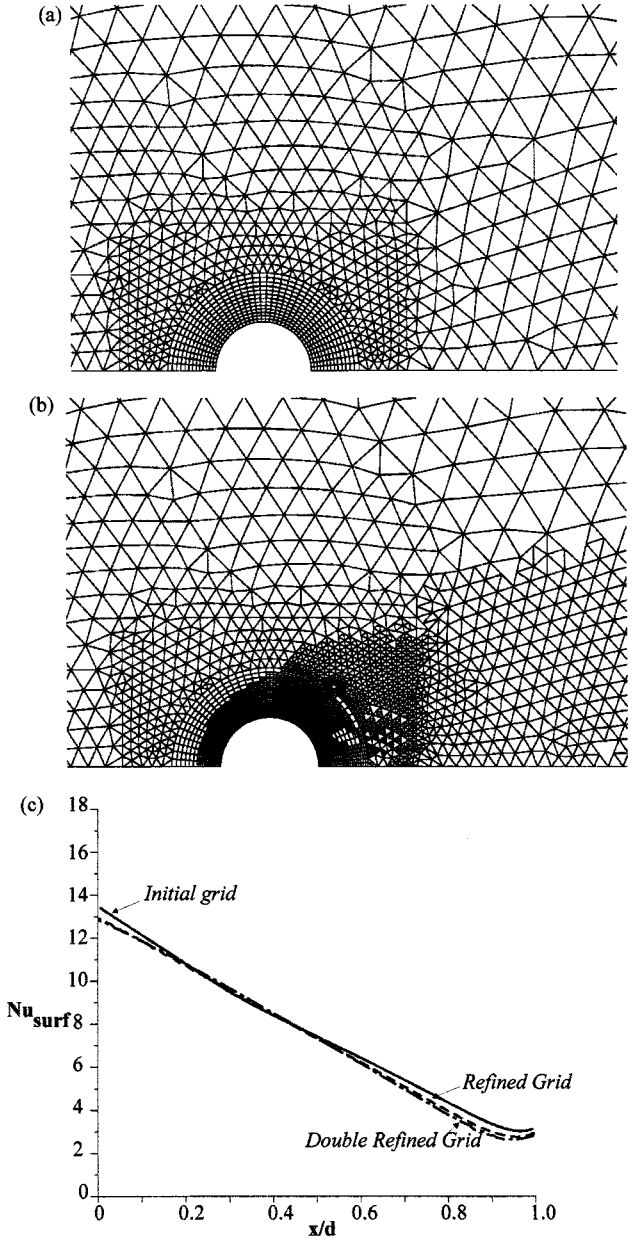

Figure 3. Demonstration of grid independence of CFD calculations.

Passing from simple (upper) to more refined grid (middle) does not change the value of *Nu* obtained for an example calculation.

Constant Surface-Temperature Simulations

Evaluation of the Ranz-Marshall correlation

One of the best known correlations for estimating the *Nu* of spherical particles is the Ranz-Marshall (RM) equation (Ranz and Marshall, 1952), where

$$Nu = 2 + 0.6\,Re^{1/2}Pr^{1/3} \tag{5}$$

and

$$Re = \frac{2R_1\rho_m u}{\mu_m},\quad Pr = \frac{\mu_m c_{p_{\text{gas}}}}{k_f}.$$

This has been used extensively in a number of modeling studies.

Given the widespread use of this correlation, and the fact that numerous authors reported difficulties in applying the RM correlation to multiple-particle situations, it was decided that it would be useful to test its validity under the conditions described earlier. This was done by examining *Nu* obtained by CFD calculations for configurations for configurations of a single particle and pairs of particles, and comparing the results with the value of *Nu* obtained using the RM correlation.

The local value of *Nu* on the particle surface is calculated from:

$$Nu = \frac{q''}{(T_{\text{surface}} - T_\infty)} * \frac{2R_1}{k_f} \qquad \text{with} \qquad q'' = k_f \left.\frac{\partial T_g}{\partial r}\right|_{\text{surface}}. \tag{6}$$

The results shown in Figure 4 for the case of a single particle in an infinite flow field are not unexpected: *Nu* increases

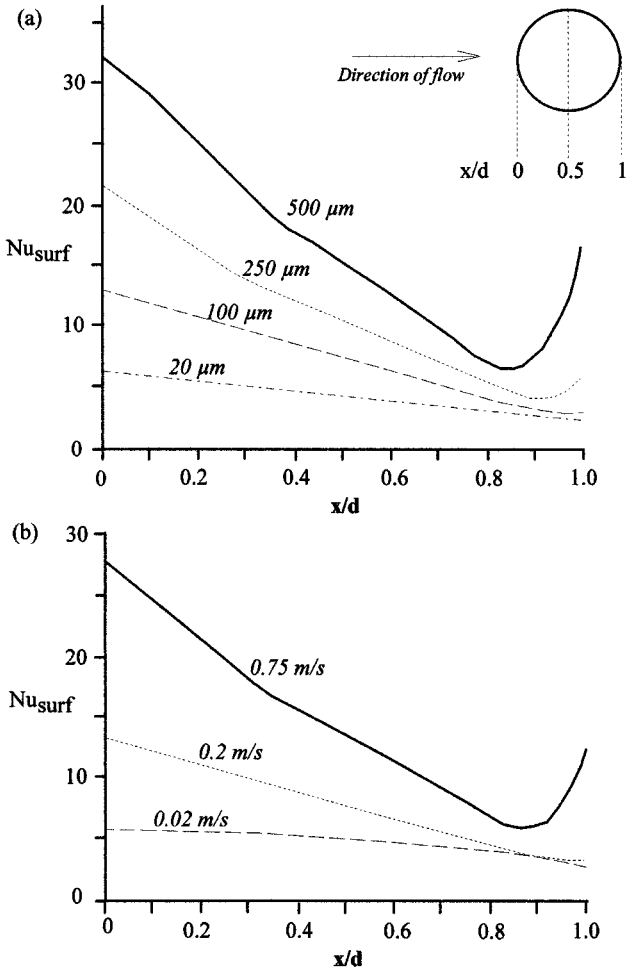

Figure 4. Surface *Nu* as a function of dimensionless axial position (*x/d*).

(a) Different particle sizes at a free field velocity of 0.2 m/s; (b) different velocities at constant particle diameter of 100 μm.

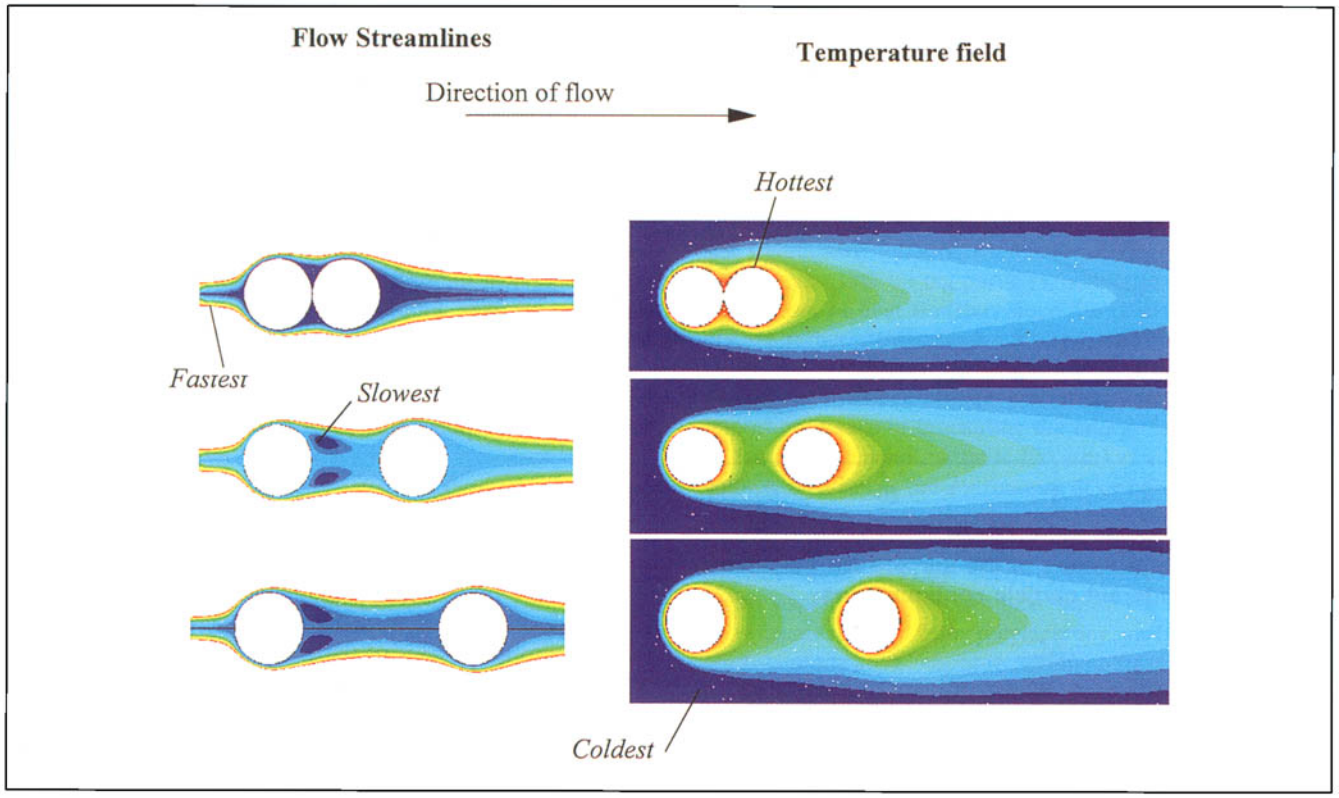

Figure 5. Velocity streamlines and temperature field around two particles as a function of their relative positions.

The gas flow (0.2 m/s) is going from left to right in this picture. Particles were 100 μm in diameter.

with particle diameter (Eq. 4a) and with velocity (Eq. 4b). That this occurs is well known, and does not merit further discussion. For the sake of conciseness, we limit the rest of the discussion in this particular section to one diameter and one velocity. The general conclusions drawn from these calculations do not change.

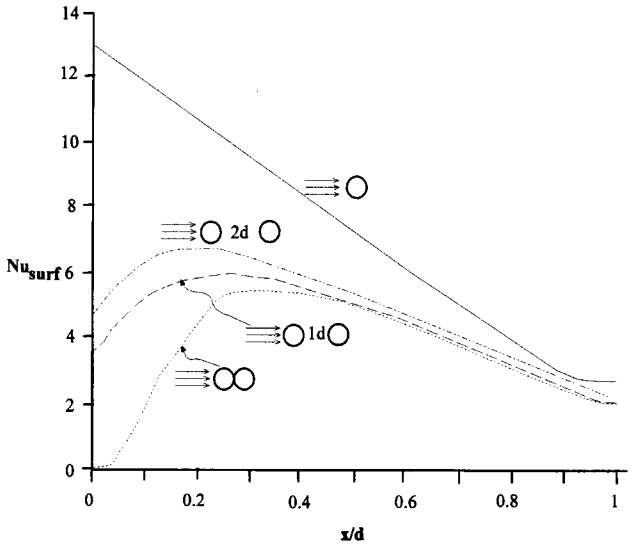

Figure 6. Surface *Nu* as a function of distance along the perimeter of a spherical particle.

In the case of two spheres separated by 0, 1, and 2 diameters, the value is for the surface of the trailing particle.

The results of CFD calculations are shown in Figures 5–7 for the case of one or two static particles of diameter equal to 100 μm, with a constant surface temperature, and surrounded by a cool gas flowing at 0.2 m/s from left to right. In this case, we assume that there is no significant aspiration of matter at the surface due to reaction. The flow and temperature fields for this case study are shown in Figure 5; the value of the surface *Nu* for the different particle configurations is shown in Figure 6; and the surface-averaged *Nu* calculated using CFD is compared with the values obtained using the RM correlation in Figure 7. In the cases where we consider two particles, the *Nu* shown is that of the trailing particle. The presence of the trailing particle has little to no effect on the *Nu* of the leading particle.

If we consider the simplest case first, that of a single sphere isolated in the well-established flow field similar to that shown in Figure 5 for two particles separated by two particle diameters, it can be seen from Figure 6 that *Nu* is relatively sensitive to the local velocity field: higher at the leading edge where the velocity is higher, and dropping off as we move along the particle, and the velocity drops off. Note that in this figure, *Nu* is plotted at the surface of the particle as a function of the dimensionless axial position, as shown in Figure 4. As in the case where we varied the free field velocity, this is not at all unexpected. However, since particles will rotate in a real environment, one should not interpret this as meaning that a different part of the same particle will experience significant

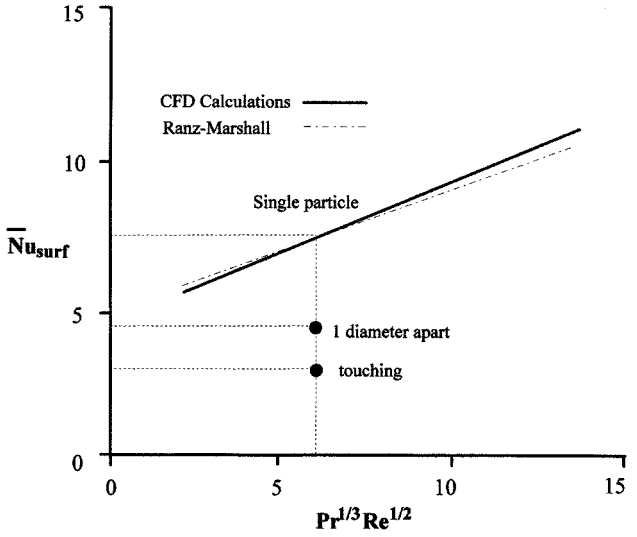

Figure 7. Average values of the surface *Nu* calculated for different particle configurations.

differences in heat transfer during the course of a reaction. A surface average value of *Nu* will thus be more representative of the heat-transfer conditions for the particle.

Figure 7 shows us that the surface average *Nu* for a single particle calculated using CFD is very similar to that calculated using the RM correlation under conditions approaching those found in a polyolefin reactor (but in the absence of any reaction). This is not overly surprising given that the correlation was developed for evaporation from a single sphere in an infinite medium, and the single sphere case does not have any complications due to the presence of bodies near the particles. Nevertheless, it is interesting to see this confirmed by other methods, and it also confirms the validity of the CFD calculations. It is also evidence of the fact that any difficulties encountered in modeling heat transfer in a polymerization reactor do not stem from the fact that this correlation is false (it is not), but rather from the fact that certain assumptions about how heat transfer occurs are probably false. This and other similar correlations are only valid in situations where particles remain relatively well-spaced. Do not forget that when it is applied to the modeling of heat transfer from growing particles, RM seems to underpredict the convective heat-transfer coefficient. This means either that heat is removed from polymerization particles by other means, or that the correlation itself is not valid (and our preliminary calculations suggest that it is valid!).

This is further corroborated by the results of the two particle calculations. The results of *Nu* as a function of dimensionless center-line position are also shown for the second particle in Figure 7 (there is very little difference between *Nu* for the leading particle and the single particle). It can be seen that the reduction in the velocity at the leading edge of the second particle (cf. Figure 5) causes the local *Nu* to decrease over most of the particle surface with respect to the value of *Nu* for a single particle, even when the particles are separated by as much as one diameter. This decrease in the leading-edge *Nu* causes the surface average value to drop. However, when the particles are separated by 2 diameters there is essentially no difference between the *Nu* for this case and the single-particle value. If we compare the resulting surface-averaged value in Figure 7 for particles that are touching, or separated by one diameter, it can be seen that the *Nu* are significantly lower than for a single sphere, or than that calculated with the RM correlation. In fact, for the touching particles, *Nu* is less than half of the value calculated with RM. This means that using the Ranz-Marshall correlation with bulk fluid velocities actually leads to an overprediction of the real Nu at the surface of the particles in closely packed systems, and thus to an overprediction of the convective heat-transfer coefficient. This in turn suggests that, in a real reactor containing a dense mass of hot particles, heat must be removed by other means during the critical instants at the beginning of the polymerization.

Effect of particle shape

The effect of particle shape and orientation with respect to the direction of flow can be seen in Figure 8, where the *Nu* at the surface of a particle is plotted as a function of dimensionless position (same meaning as in Figure 4). The ratio of the major to minor axes of the ellipsoids was 2:1 (the minor axis being set at 100 μm).

It can be seen here that the *Nu* at the leading point (that is, where the gas hits first) of the different particles is significantly affected by the shape and orientation of the particles. However, the lowest value is still relatively high, and this influence quickly disappears. Furthermore, although *Nu* is slightly lower for more particles aligned with the direction of flow, it is easy to imagine that the value of *Nu* averaged over the surface is quite similar in all cases. Also, particles in real flow situations probably rotate with respect to the direction of flow. We can therefore conclude that in so far as the heat-transfer coefficient for the particles studied here is con-

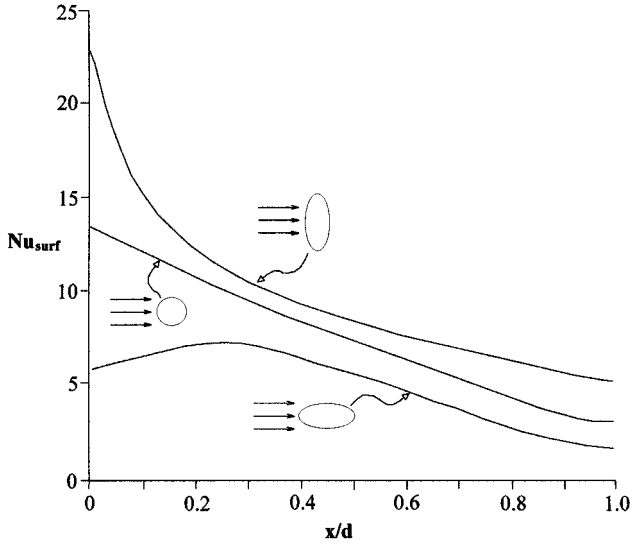

Figure 8. Effect of particle shape and orientation on surface *Nu* number at a linear gas speed of 0.2 m/s for a sphere with a diameter of 100 μm and for 2 ellipsoids of the same volume average diameter.

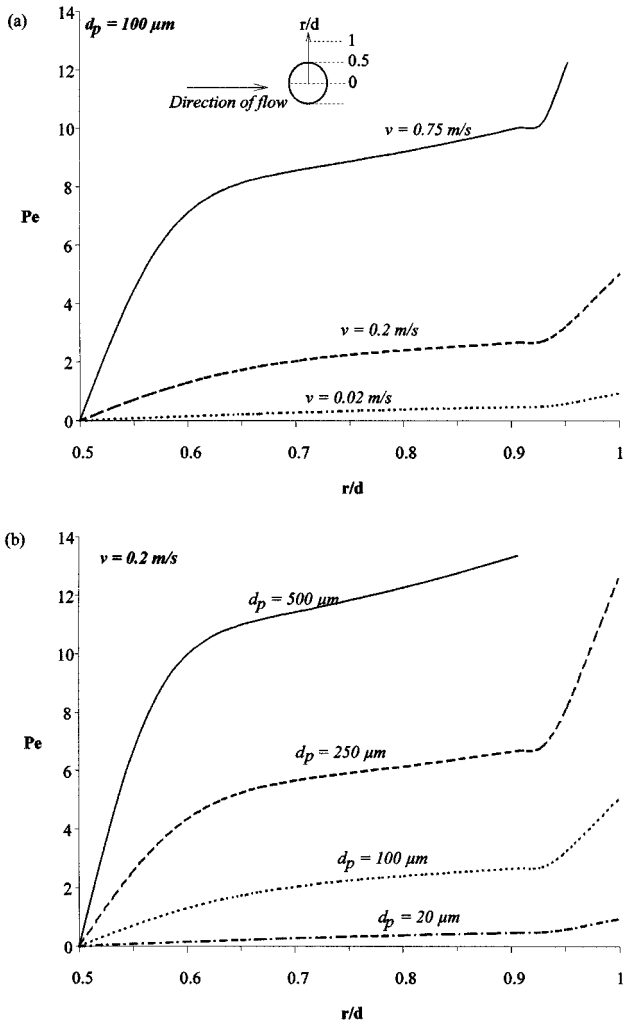

Figure 9. Variation of heat transfer *Pe* above particle surface as a function of dimensionless radial position.

(a) Varying velocity and a fixed particle size; (b) varying particle sizes and a fixed velocity.

cerned, the shape and orientation of the particles, while not negligible, have only a secondary influence compared to the particle–particle interactions shown earlier. It can be seen from Figures 4, 6, and 8 that the average value of *Nu* for round and elliptical particles is similar. This suggests that the RM, or any other correlation, can be applied to aspherical particles without too much difficulty, but, of course, with the same restrictions as mentioned before. Therefore, we will not consider the influence of particle shape in what follows.

One final result from the constant surface-temperature particles is shown in Figure 9, where we can see the variation of the heat-transfer Peclet number (*Pe*) for a single particle in an infinite flow stream as a function of dimensionless radial position at the particle surface in the direction normal to the main flow vectors. The heat transfer *Pe* is defined as

$$Pe_H = \frac{L\rho u c_p}{k_f} = \frac{\text{convective heat transfer}}{\text{conductive heat transfer}},$$

where k_f is the thermal diffusivity of the gas, c_p its heat capacity, u the local velocity, and L a characteristic length scale (here taken to be the average size of the control volume used in the numerical integration scheme. Figure 9a shows the results for varying free stream velocities at a fixed particle diameter of 100 μm, and Figure 9b shows the influence of varying particle size at a fixed free stream velocity of 0.2 m/s. It is immediately evident (and to be expected) that particle size significantly influences the value of *Pe*. The results shown here suggest that for big particles, convection is the dominant mechanism of heat transfer, since the particle boundary layers are rather small compared to particle size. The opposite is true for small particles, where for the 20-μm particles, especially at low free stream velocities, conduction is a very important means of evacuating the energy from the particles. In fact, for the small particles (20 μm) at a fixed free stream velocity of 0.2 m/s, the *Pe* remains at or below 1 for over one particle radius above the surface. Since we have previously seen that the presence of particles in the reactor can perturb the free stream velocity ''seen'' by neighboring particles, it is highly likely that convective heat transfer is not the only way to evacuate energy from polymerizing particles. This result lends quantitative support to hypotheses published by McKenna et al. (1995a,b), where the authors did an order-of-magnitude calculation to show that, in certain cases (small particles, low velocities), conduction might play an important role in heat transfer. This point is explored below in more detail.

It should be noted that while a constant surface temperature is not necessarily reflective of conditions in a reacting system where temperatures can depend on a large number of variables, this configuration was chosen in order to explore some limiting cases and to obtain information on the validity of the Ranz-Marshall correlation. This will become clear from some of the case studies presented below. Such a simplified problem structure is therefore probably acceptable, at least to draw conclusions about the fact that it is unlikely that convection alone can explain how the heat is removed from the particles, and the effect of particle shape.

Constant Heat and Volumetric Flux Conditions

It is probably more appropriate to study flow systems where we have a constant heat flux at the particle surface, or, even better, constant rate of heat production per unit volume throughout a particle.

Constant surface heat flux

It is a relatively simple matter to estimate heat fluxes based on ''observed'' reaction rates. It is simply the product of the observed rate of reaction times the heat of polymerization times the mass of catalyst per particle, divided by the surface area of the particle:

$$\hat{Q}_{\text{surf}} = \frac{R_p \rho_{\text{eff}} \frac{4}{3}\pi R_o^3}{4\pi R^2} \Delta H_p. \qquad (7)$$

If one accepts that the density of a catalyst particle is on the order of 1 g/cm^3, that of a growing polymer particle is ap-

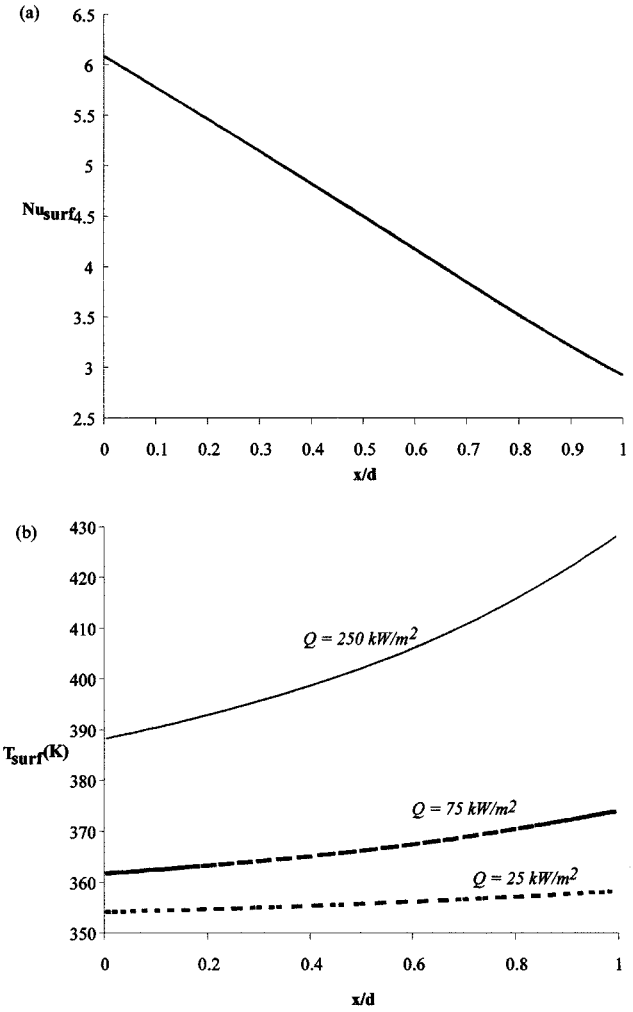

Figure 10. Evolution of *Nu* and surface temperature of a single sphere as a function of position along the perimeter for different heat fluxes.

Note that the 3 curves of *Nu* as a function of *x/d* are indistinguishable.

proximately 0.5 g/cm^3, that the heat of polymerization of ethylene is on the order of 100 kJ/mol and that the particles are roughly spherical, it is easy to calculate average heat fluxes that correspond to observed reaction rates. If we consider a range of reaction rates from 5000 g to 50,000 g polymer per g catalyst per hour, the heat flux for relatively small particles (20 μm) at the beginning of the reaction should range from about 20 to 200 kW/m^2, respectively, and by the time they get to be 100 μm (starting from 20 μm), the range of heat fluxes is on the order of 0.5 to 20 kW/m^2. We therefore consider a range of values of constant surface heat fluxes from 25 to 250 kW/m^2 as being representative of a wide range of (reasonable) polymerization conditions.

The evolution of *Nu* and of the surface temperature for a single sphere as a function of dimensionless axial position is shown for different heat fluxes in Figure 10 for relative particle–gas velocities of 0.2 m/s. The surface temperatures were calculated by imposing a constant heat flux at the particle surface and estimating the corresponding value of *Nu*. If we assume that heat removal is by convection only, it can be seen that surface temperatures can be very high for small (20 μm) particles that generate heat fluxes of 250 kW/m^2 (note that the melting point of polyethylene varies from 130°C down to about 100°C, as the comonomer content increases). This has obvious implications in reactor stability and control, although it should be noted that these heat fluxes are valid only at the very beginning of the reaction (this kind of temperature can only be reached in simulation!). As can be seen in Eq. 7 the heat flux varies as one over the particle radius, which increases very rapidly during the early stages of the polymerization. So if we manage to pass through the first few moments of the polymerization, the specific heat flux per square meter will continually decrease, as will the surface temperature.

However, as we saw before, particle–particle interaction cannot be neglected, since it has a significant effect on local *Nu* values, especially in the event that particles are touching. Let us consider the case of two small particles, representative of fresh catalyst. Results of CFD calculations with different heat fluxes for two touching particles with diameters of 20 μm are shown in Figure 11. As one would suspect, the point where the two particles are in contact is the hottest, regardless of the heat flux. In the case of the small highly active particles, the surface temperature drops rapidly as we move along the particle perimeter before increasing slightly in the recirculation zones at its rear. Of course, a value of 250 kW/m^2 is very high and, as we stated earlier, it drops rapidly, so it is very unlikely that the surface temperature of a particle really attains 650 K. In fact, as the temperature increases much above the melting point of the polymer, the pores would fill with molten polymer. This would have the effect of increasing mass-transfer resistance, thereby cutting off the monomer supply to the active sites, and the reaction would stop well before the surface temperature of a particle attains 650 K, as predicted in this figure.

Note that *Nu* as shown in Figures 10 and 11 does not depend on the surface flux under the conditions that we have imposed here (density, k_f, viscosity, etc., independent of temperature). This is of course not entirely rigorous since physical properties are usually moderate functions of temperature. However, as we explore the order of magnitude effects here, there seems to be no need for highly detailed physical models, and any slight alteration to parameters such as viscosity and thermal diffusivity will not have any significant effect on the final conclusions.

However, the results of Figures 10 and 11 suggest that hot spots really can form between two particles of the same size that are in contact with each other. This is reinforced by the fact that even for significantly lower values of the heat flux—values that are encountered for periods longer than a few seconds—hot spots with temperatures higher than the melting point of polyethylene can form at the interface between two particles in contact. This at least explains how meltdown might occur in reactive situations: two small, highly active particles collide, then rest together long enough for meltdown to occur. This forms a ''pseudoparticle'' with a larger value of R_o than the first two particles, thereby increasing the heat flux per unit surface, which increases the temperature, and so on. However, for particles with lower heat fluxes—those that correspond to larger particles—the

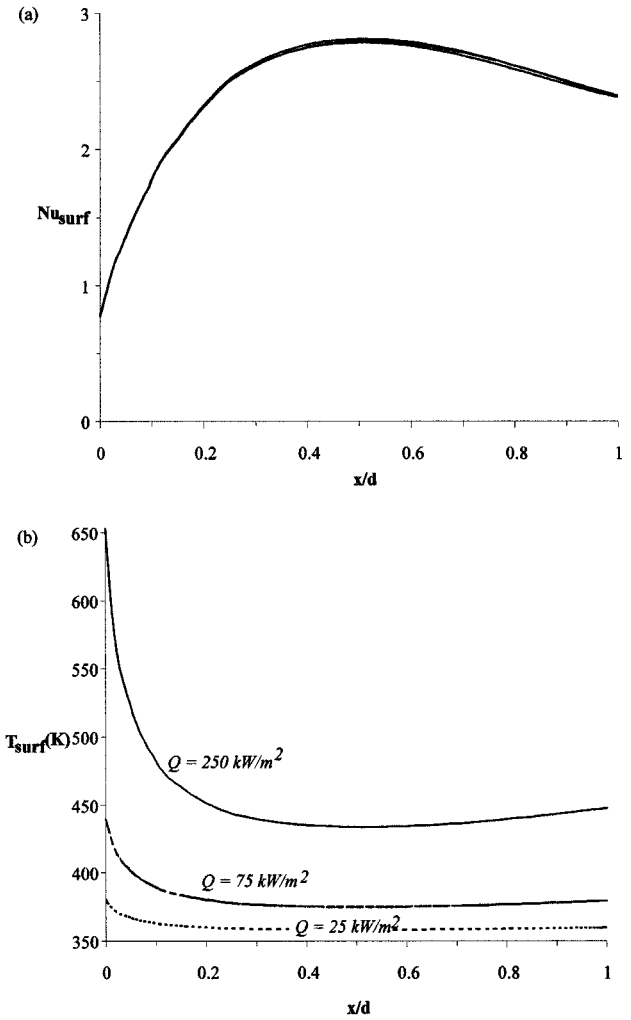

Figure 11. CFD calculations (Nu_{surf} and T_{surf}) with different heat fluxes for two touching particles with diameters of 20 μm.

As in Figure 10, the value of *Nu* is independent of the flux.

temperature rise is not particularly important. So one would suspect that larger particles will not melt when they come into contact, even if they are highly active, since the heat flux per unit surface is relatively low.

Up to this point, we have only considered particle–particle interaction for particles of the same size. In the final series of simulations of constant heat-flux conditions, we examined the interaction between large and small particles with the configuration shown in Figure 12. In a continuous reactor, one will frequently find very large particles near the end of their residence in the reactor alongside small, freshly injected particles. As we saw earlier, the specific heat flux per unit surface is so low for large particles that their surface temperature is close to that of the free stream flow. For this reason we decided to set the surface temperature of the large particles in this configuration equal to 350 K, the same as the bulk fluid. We then ran a series of simulations with small particles having different initial heat fluxes (that is, initial activities) of 75, 150 and 250 kW/m^2 (which correspond to observed activities of 18 kg/g/h, 36 kg/g/h, and 60 kg/g/h). The particles were allowed to "grow" from an initial diameter of 25 μm, to 50, 100 and 250 μm. The effect of this was to reduce the initial value of the surface heat flux by a factor of 4, 16 and 100. The results of this series of simulations is shown in Figure 13 in the form of the surface temperature of the small particle as a function of its dimensionless axial position (relative velocities 0.2 m/s).

As one should expect by now, the surface temperature of the small particle diminishes rapidly as the particle gets larger. Also, given the fact that the larger particle masks the smaller ones from the bulk flow, the *Nu* at the surface of the smaller particles is lower than for similar sized particles (see Figure 4), and the surface temperature is correspondingly higher for the middle particle in the configuration in Figure 12 than it is for a single particle on its own size. However, given the relatively constant (almost zero) flow field in the vicinity of the small particle (see Figure 14), the surface temperature varies little as one moves along the surface of the small particle. Finally, only the low-activity particle seems to have a relatively acceptable surface temperature before it starts to grow. The average surface temperature for the 25-μm particles is 383, 416 and 461 K (remember the melting point of high-density polyethylene is on the order of 400 to 405 K) for surface fluxes of 75, 150 and 250 kW/m^3, respectively. As the particles grow, the average surface temperatures are 352, 355 and 359 K for the same fluxes. The initial particle diameter is admittedly a bit high in this case—one might expect modern catalyst particles to be more on the order of 12–20 μm in diameter. Nevertheless, these simulations still show that large particles, even if they are relatively cold, have the effect of masking small particles from the free stream flow, thereby increasing any difficulties associated with the removal of heat from them (if they are not touching!), and that it is indeed in and around the small particles that heat transfer must be better studied.

Again, this series of calculations is a simplified picture of what should occur in a reacting system, and we have assumed here that the particle center does not heat up. This restriction will be lifted in subsequent simulations, but the results obtained here will help us to identify systems where more detailed calculations should be performed.

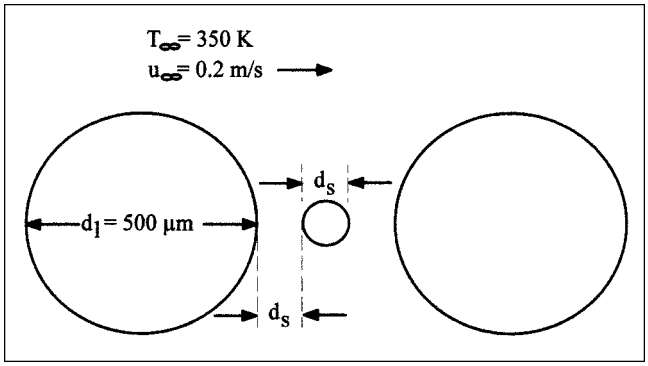

Figure 12. Configuration of particles for 3 particle simulations.

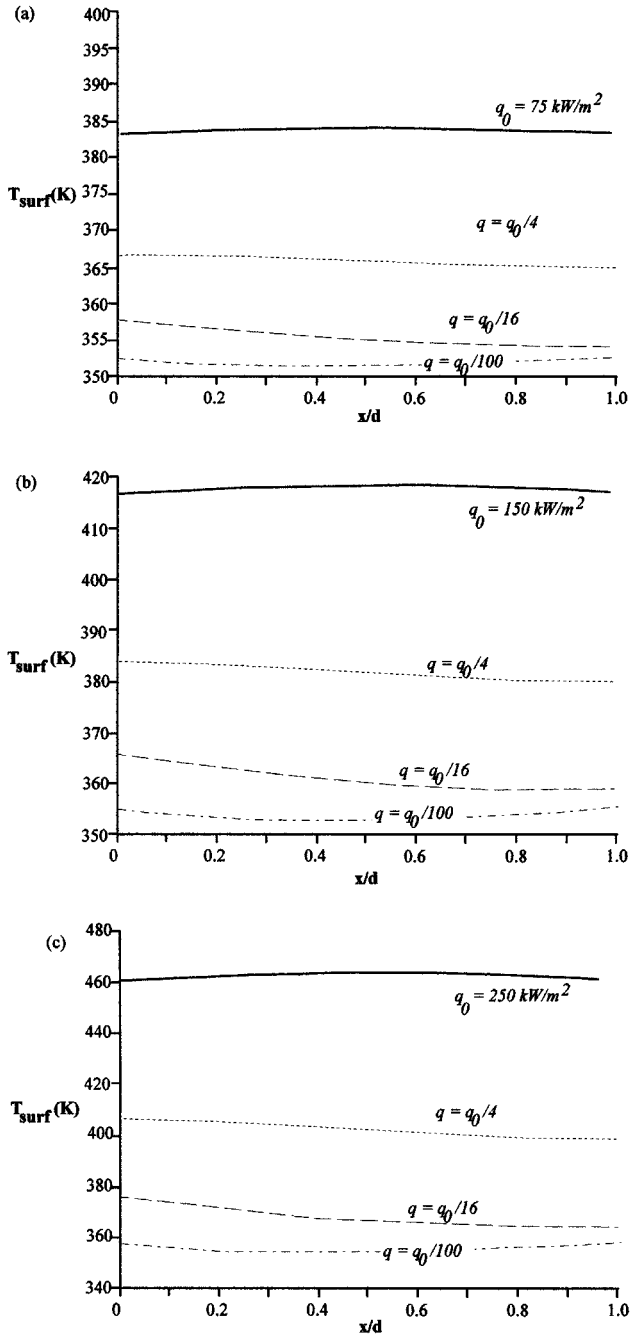

Figure 13. Surface temperature of small particle in Figure 12 as a function of initial rate of heat generation and particle "growth."

Heat flux was divided by 4, 16, and 100 to similate diameters of 2, 4 and 10 times the original particle diameter.

Constant volumetric heat flux with intraparticle conduction

The final series of simulations to be presented here is that of particles with constant heat flux per gram of catalyst (effective heat flux inversely proportional to the particle volume) and the incorporation of the possibility of conduction of energy within the solid body. The previous simulations using constant surface temperature, then constant surface heat flux, were used to isolate the range of particles sizes, configurations, and conditions that warranted further investigation. In this last section, Eqs. 3 and 4 were solved for the gas phase as above, and a third equation describing conduction in the solid body was added:

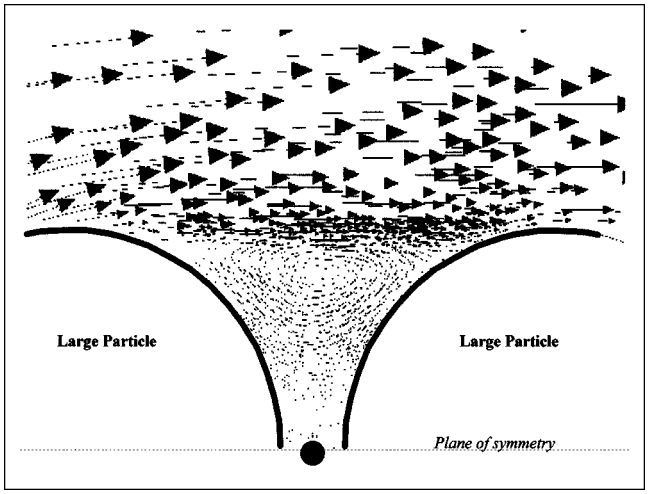

Figure 14. Flow field in the vicinity of small particle in Figure 12.

Velocity of gas is proportional to the length of the arrows.

$$\frac{\partial}{\partial t}\left(\rho c_{p,s} T_s\right) = \frac{\partial}{\partial x_i}\left[k_{e,s}\left(\frac{\partial T_s}{\partial x_i}\right)\right] + \hat{Q}_{\text{vol}}. \tag{8}$$

For all of the simulations that follow, we used a solid phase density of 900 kg/m^3, a thermal conductivity of 0.117 W/m/K, and a specific heat of 2.15 kJ/kg/K. The volumetric heat flux from a particle is given by

$$\hat{Q}_{\text{vol}} = \frac{R_p \rho_{\text{eff}} \frac{4}{3}\pi R_o^3}{\frac{4}{3}\pi R^3}\Delta H_p. \tag{9}$$

If we take the same parameter values as before, the volumetric heat flux for a 20-μm particle at the beginning of the reaction is about 5×10^6 kW/m^3 for an observed activity of 5,000 g/g/h, and 5×10^7 kW/m^3 for 50,000 g/g/h. As the particle grows, the heat flux will drop as one over the ratio of the original to the new particle diameter to the power of three. For example, if we choose a value of the volumetric heat flux for small particles of 10 μm in radius on the order of 10^7 kW/m^3, it is reasonable to take values on the order of 640 for particles with a radius of 250 μm. Note that the observed rate of polymerization in terms of grams of polymer per gram of catalyst per hour in both particles would be the same. The fact that the active sites are "diluted" in the growing particle by the polymer produced means that, although the quantity of active sites per particle remains constant, the concentration of active sites, and thus the rate of heat generation per unit volume, drops. As we will see below, this is an important point.

To begin with, we evaluated the same particle arrangement as in Figure 12, with only very slight changes in particle sizes: the small particle was taken to be 20 μm in diameter instead of 25, but the larger particles remained at 500 μm in diameter. Particle heat fluxes were taken as 4×10^7 kW/m^3 for the small particle and 2×10^3 kW/m^3 for the large ones. The free stream velocity was taken as 0.2 m/s, and bulk temperature was set at 350 K.

The flow field is evidently very similar to the one in Figure 14, where the large particles shield the small one from the flow. This, combined with the extremely high heat flux in the small particles, has the effect of causing the overheating of the small particles. This can be seen from the graph in Figure 15, where the simulations predict a core temperature of 436 K for the small particles—way over the melting point of even polypropylene, and thus not physically realistic. Nevertheless, this shows two things: (1) the results of the constant surface flux calculations are quite reasonable. There is only a small temperature gradient inside the particles under these conditions. The major gradient is between the small particle and the surrounding fluid. Of course, overheating in a reacting particle would push the reaction rate higher and higher, which would obviously have the effect of creating larger temperature gradients within the particle. (2) If particle–particle interactions are to play a role in heat-transfer removal, it is not sufficient for the small particles simply to be in the vicinity of

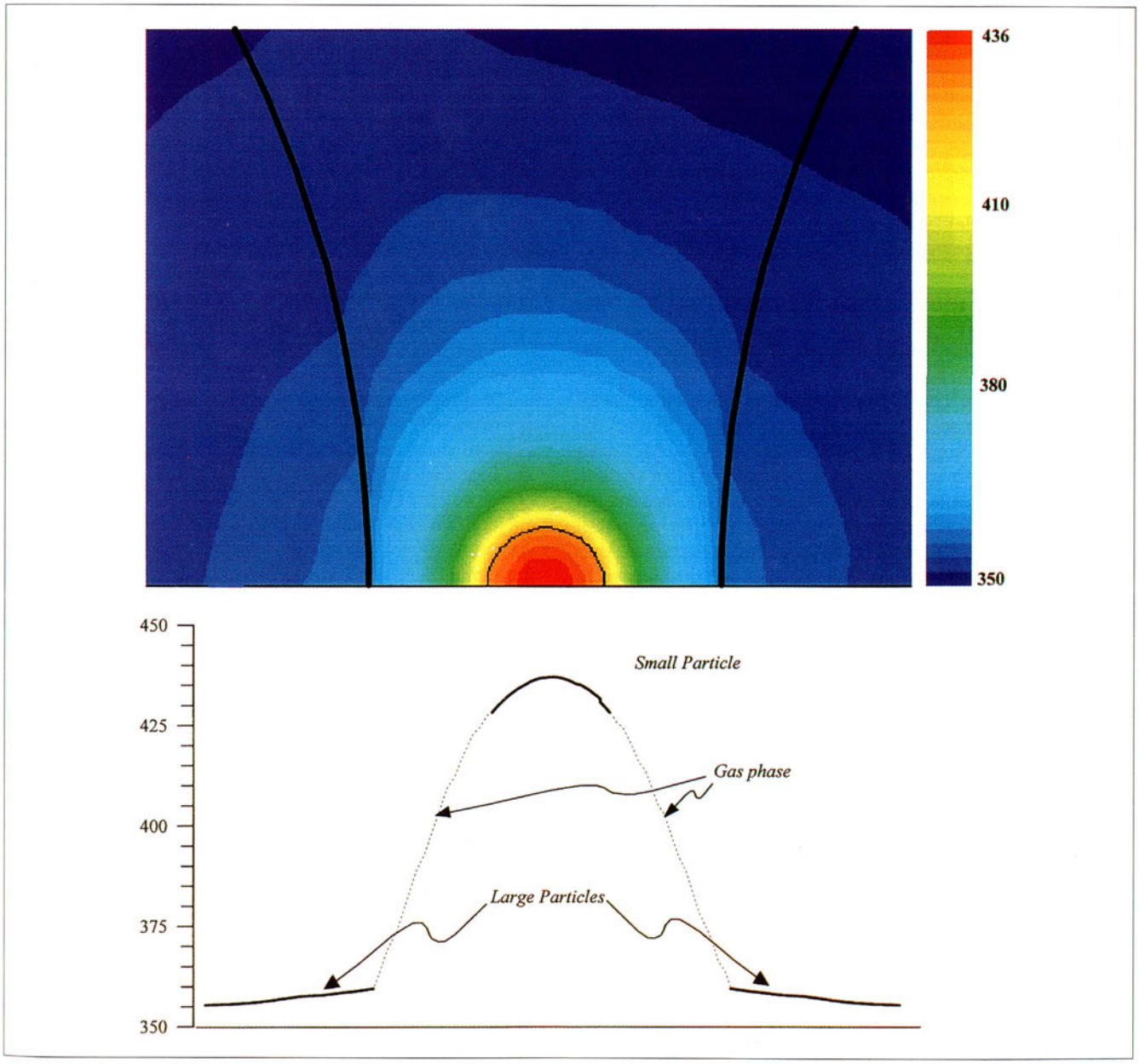

Figure 15. Temperature contour map for case of one small particle ($d_p = 20$ μm) surrounded by 2 large ones ($d_p = 500$ μm).

Heat fluxes are 4×10^7 kW/m^3 for the small particle and 2×10^3 kW/m^3 for the large ones. Thick black lines indicate large-particle boundaries.

large ones. In fact, it can be seen that the large particles are hardly heated at all by the small one, even at a distance of only 20 μm. This can be seen in Figure 15, where the center-line temperatures in the simulated system are shown as a function of position. It is interesting to note the very small temperature gradient inside the larger particle when compared with the two others in the system.

One last point that seems useful to look at is the time it takes for the steady-state temperature profiles to develop in this system. It should be pointed out that for reasons of economy, all of the results presented up to this point were for steady-state calculations. In order to verify that this is a valid approach, the calculations in Figure 15 were repeated in transient mode. It can be seen from Figure 16 that it takes only 0.025 s for the surface temperature of the small particle to reach 99% of its steady-state value, and becomes identical to the steady-state value at 0.5 s. For this reason, it seems reasonable to accept the conclusions drawn to this point with the steady-state calculations.

In the earlier parts of this article, we saw that:

- Single particles in a free stream might overheat if heat generation rates are comparable to those of a moderately active olefin polymerization, but generally will not
- Small particles overheat more than large ones, even if small and large particles have the same rate of polymerization
- If two small particles touch, the contact point will overheat
- Large particles can mask small ones from the cold gas stream, and thus lead to their overheating.

Although these conclusions provide us with some useful information, they seem to represent (to a certain extent) the quantification of some of the objections raised by McKenna et al. (1995a,b) to earlier articles on the modeling of heat transfer in polyolefin processes. We still do not understand why all of the heat that is produced during the course of these reactions is removed, because, although certain models and simulations would have it otherwise, we do manage to

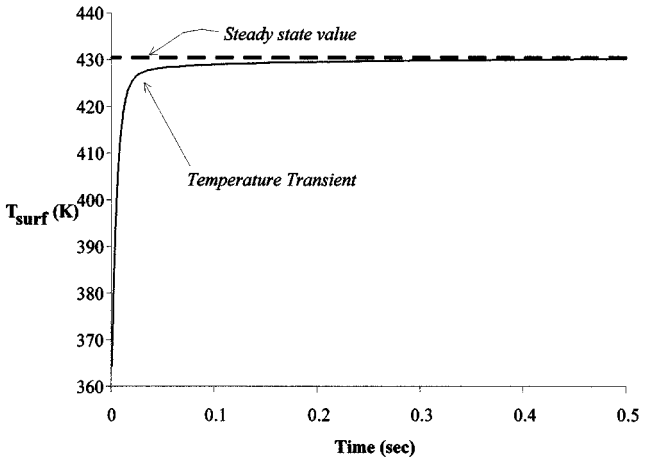

Figure 16. Difference between steady state and transient calculations.

A cold particle injected into this stream that begins to react immediately will reach 99% of the steady-state temperature in less than 0.025 s.

polymerize ethylene at rates on the order of several tens of thousands of grams per gram per hour in gas-phase fluidized beds. As we pointed out earlier, one of the major weak points of previous modeling efforts is that particle–particle and particle–wall collisions are not included in polyolefin models (although other workers such as Martin (1979, 1984) have tried to quantify this effect).

For this reason, it was decided to investigate whether collision between the particles improved or worsened the situation. We therefore defined a series of test cases that involve small particles in contact with larger ones, and in contact with heat-transfer surface areas such as the reactor wall. Given the results presented earlier, it did not seem particularly useful to continue modeling interaction between two small particles.

The case studied here consists of a large and small particle that touch each other at a single point. The small particle ($d_p = 20$ μm) is said to be upstream with respect to the gas flow (relative velocity of 0.2 m/s), and the large one ($d_p = 800$ μm) is behind it. Both the mesh and the temperature contours are shown in Figure 17a. Both solid zones (catalyst and polymer) are assumed to have identical properties apart from different heat release: heat fluxes are 4×10^7 kW/m^3 for the small particle and 625 kW/m^3 for the large one. It is interesting to note here that instead of observing a hot spot at the contact point, the temperature contours shown in this figure indicate that the small particle is instead cooled down by being in contact with the larger one. Consequently, the maximum temperature in the system is inside the small particle, rather than at the interface. Furthermore, the hottest point in the system, just to the left of center in the small particle, is approximately 390 K—less than the melting point of a typical high- to medium-density polyethylene despite the fact that the heat flux in the small particle corresponds to an activity on the order of 50,000 g/g/h!

Note that the simulation in Figure 17a (where the gas flow was coming from left to right) was rerun for a gas flow coming from the other direction. Although the results are not shown here, it was found that the hottest spot in this second configuration (that is, where the small particle is hidden from the flow by the big one) is equal to 392.4 K, a similar value as for the case where the large particle does not directly hide the small one. This observation is simply due to the fact that the small particle is of the same order of size as the large particle boundary layer, so convective effects at the particle surface are essentially negligible. This is a very significant result! In fact, this strongly suggests that heat transfer from very hot particles in packed systems can occur to a large extent by conduction.

Note that the results in Figure 17a are shown at a time of 0.3 s. As we saw earlier, it takes very little time to reach steady state in a dynamic simulation. Of course, it remains to be said just how long two particles such as these remain in contact, and how frequently they collide. Furthermore, the transient calculations assumed that the small particles had an initial temperature of 350 K everywhere. However, it should once again be stressed here that the principal objective of these simulations is not to provide an exact model of a polyolefin polymerization, but rather to help us to quantify some of the principal phenomena that might play a role in heat transfer in these systems, and to understand why we are able

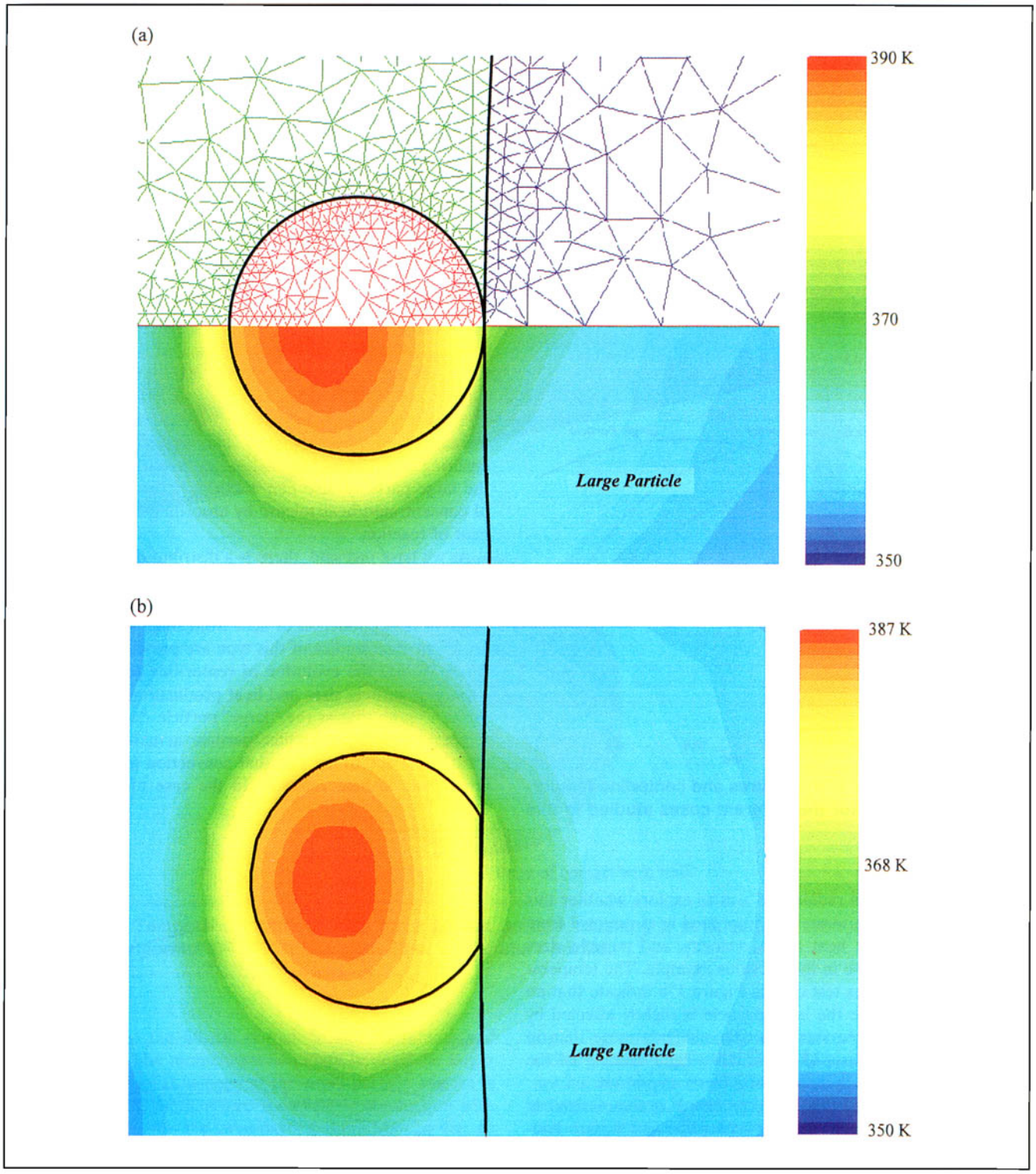

Figure 17. Coupled flow-solid heat-transfer problem.

(a) Two touching, conducting bodies (CFD grid on upper portion, temperature profile on bottom); (b) two touching, conducting bodies with a contact surface area 5 μm in diameter.

to remove heat that traditional models say we cannot get out of the particles.

The next test case is also concerned with the interaction of the particles shown in Figure 17b. In a more realistic situation, it is very unlikely that most of the particles with which we are dealing in the case of olefin polymerization have very smooth, uniform surfaces. For this reason it is also unlikely that two particles coming into contact will touch only at a small point. Therefore, we chose to simulate the case of two particles touching with a larger contact area in the shape of a

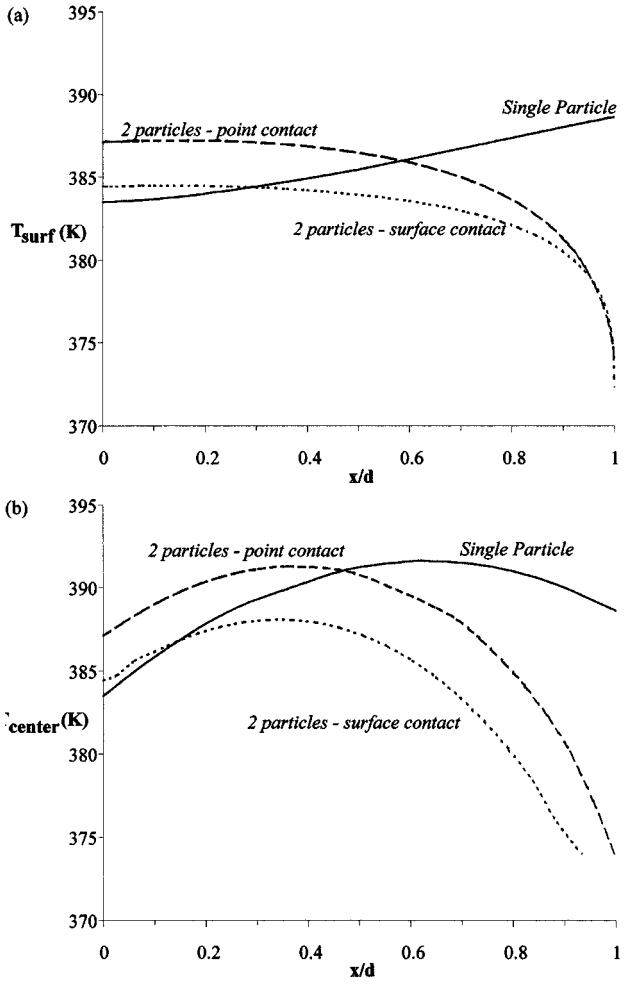

Figure 18. Surface temperatures and centerline temperatures for the different cases studied in this work.

circular plane with a radius of 5 μm to explore whether this type of contact deteriorated or improved heat removal from small particles. The heat fluxes, velocity, and particle sizes are the same as those in the previous example. The temperature contours for this test case in Figure 17b indicate that an extended area inside the large particle is slightly affected by heat coming from the small particle—slightly more than in the point contact case. However, this slight heating of the large particle generally is not particularly important.

The importance of this contact heating is summarized in Figure 18, where we can see the center-line and surface temperatures for the point-contact and surface-contact examples, compared to the results of the same simulation for a single particle in a free gas stream. Note that the ''best'' heat transfer is obtained in the case where there is a contact surface. Generally speaking, the point-contact and single-particle simulations reveal very similar temperature profiles, with the average temperature inside the particle with the point contact being just slightly lower. This is interesting since it should not be forgotten that the local velocity profiles in these two cases are very different. In the case of the single particle, the velocity near the particle surface is relatively high, which improves local heat transfer and aids in the cooling of the particle. On the other hand, if a single particle is ''shielded'' by a large particle that nevertheless does not touch it, it can significantly overheat. This was demonstrated by the previous set of simulations using constant heat flux (4×10^7 kW/m^3 roughly corresponds to a surface heat flux of 200 kW/m^2 for a 20 μm particle) in Figure 12. Thus the small particles that overheat in the ''not touching'' geometry of Figures 11 and 12 are sufficiently well-cooled, even at high activities, by simple contact with large particles.

This helps to quantitatively explain the need to add inert powder particles when starting up a batch reactor. In a continuous reactor such as an FBR, there is a wide distribution of particle size in the reactor at steady state. It is therefore quite likely that there are enough large particles to absorb the heat of the smaller ones when catalyst or prepolymer particles are injected into the reactor. On the other hand, in a batch reactor all particles are more or less the same size at all times during the reaction. Therefore, in addition to helping ensure even distribution of the catalyst particles (that is, ensuring that two small particles do not come into contact), the large particles also help us to get over the initial hurdle of concentrated heat release by absorbing a good part of the heat of reaction.

As we have just said, there is a distribution of particle sizes in continuous reactors. It is therefore of interest to look at the effect of varying the relative length scales on the importance of the conduction of heat from small to large particles. Different case studies of this type are presented in Figure 19 where we see the evolution of center-line temperature for a variety of particle sizes and heat production rates. It is interesting to note that as the ''large'' particle decreases, the core temperature of the smaller particle actually drops. This is most likely due to the fact that convection plays a larger and larger role in heat removal. In the case of the 20–800-μm

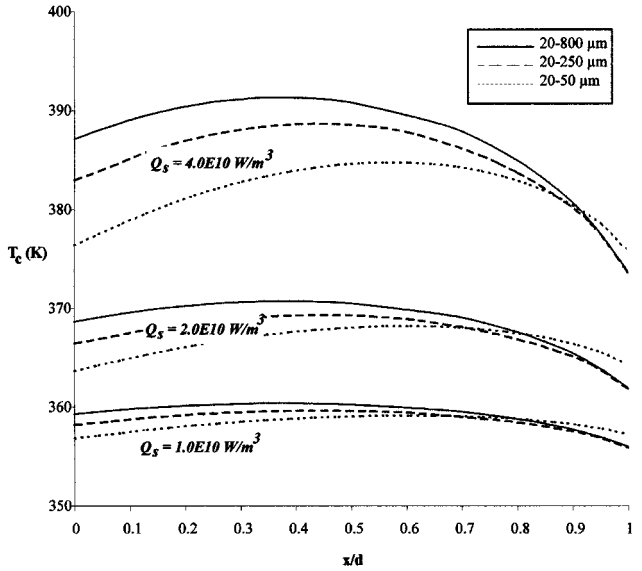

Figure 19. Centerline temperature profiles for the case of 2 particles touching at a single point—effect of relative particle sizes on centerline profiles.

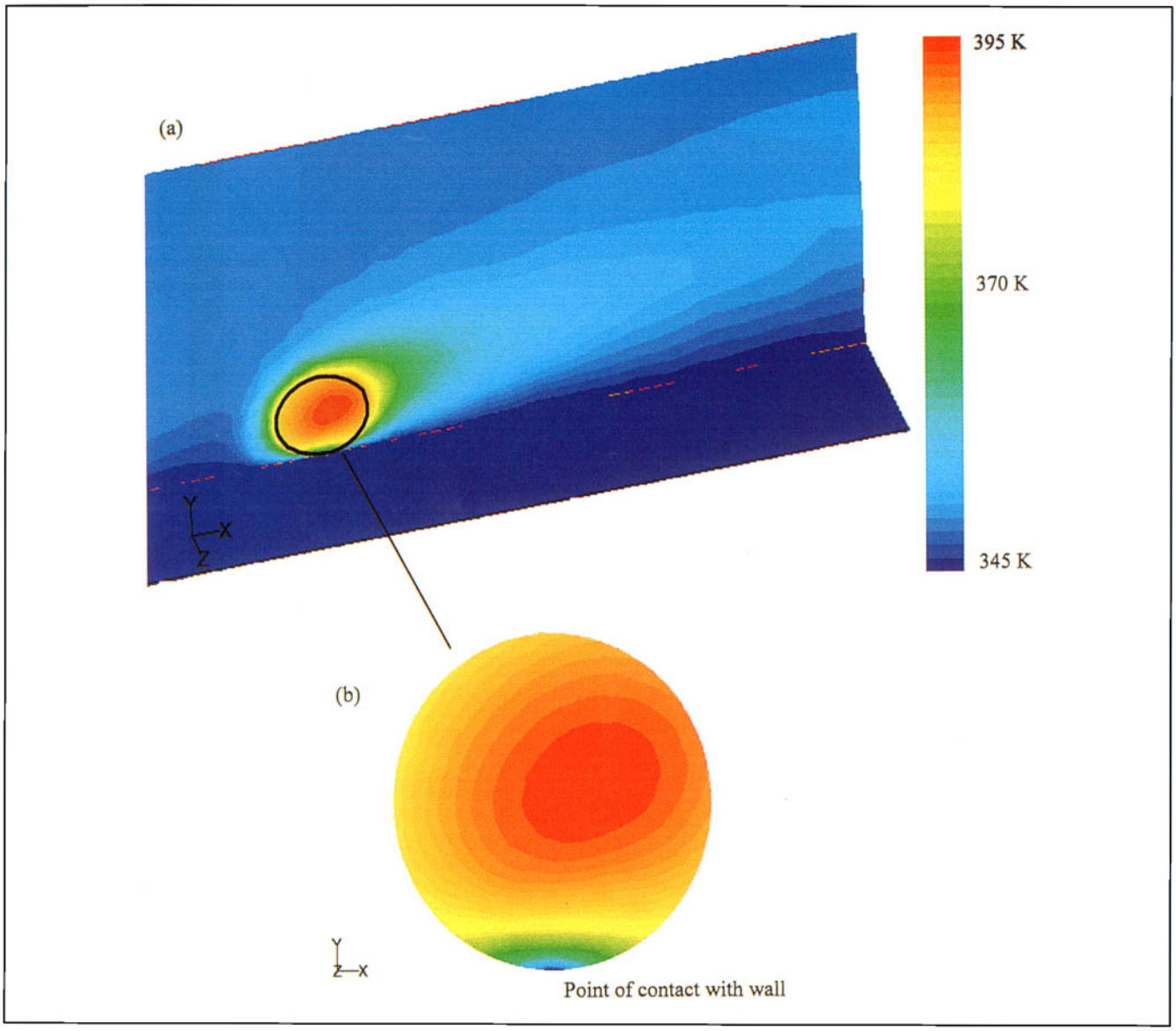

Figure 20. (a) Temperature contour map for a 20-μm particle touching a cold surface such as the reactor wall (temperature = 345 K); (b) closeup of temperature profile.

pair of particles, the 20-μm particle is, for all intents and purposes, inside the momentum boundary layer of the larger particle and the local velocity at the small particle surface is very low. All heat is therefore removed by conduction with the larger particle. As the large particle diminishes in size, its boundary layer gets smaller and smaller, and the gas velocity at the small-particle surface increases. This helps to cool the particles to a certain extent. However, once the two small particles are more or less the same size, hot spots can form as shown earlier. This is a very interesting explanation for how meltdown, or particle agglomeration can occur in an FBR reactor for the polymerization of ethylene or propylene in the gas phase.

In the final series of test simulations, we examined the influence of the interaction between a hot particle and an inert (that is, nonpolymerizing) object such as the reactor wall using 3-D geometry whereby the sphere (particle) with 20-μm radius is touching the wall at a single point. A full 3-D grid is needed in this case, and the calculations become much more time-consuming. However, from a physical point of view, this test case differs from the 20–500-μm case, essentially in the choice of boundary conditions. In the case of two particles treated as conducting bodies, the larger particle has such a low heat flux that it is almost inert. The major difference between an essentially inert polymer particle and the reactor wall is that, the reactor wall (assumed to be made of stainless steel) is a much better conductor of heat than a polymer particle.

If we assume that the reactor wall is a body with a constant surface temperature of 345 K, we obtain the temperature contours shown in Figure 20 for a 20-μm-diameter particle with a constant volumetric heat flux of 4×10^7 kW/m^3. Obvi-

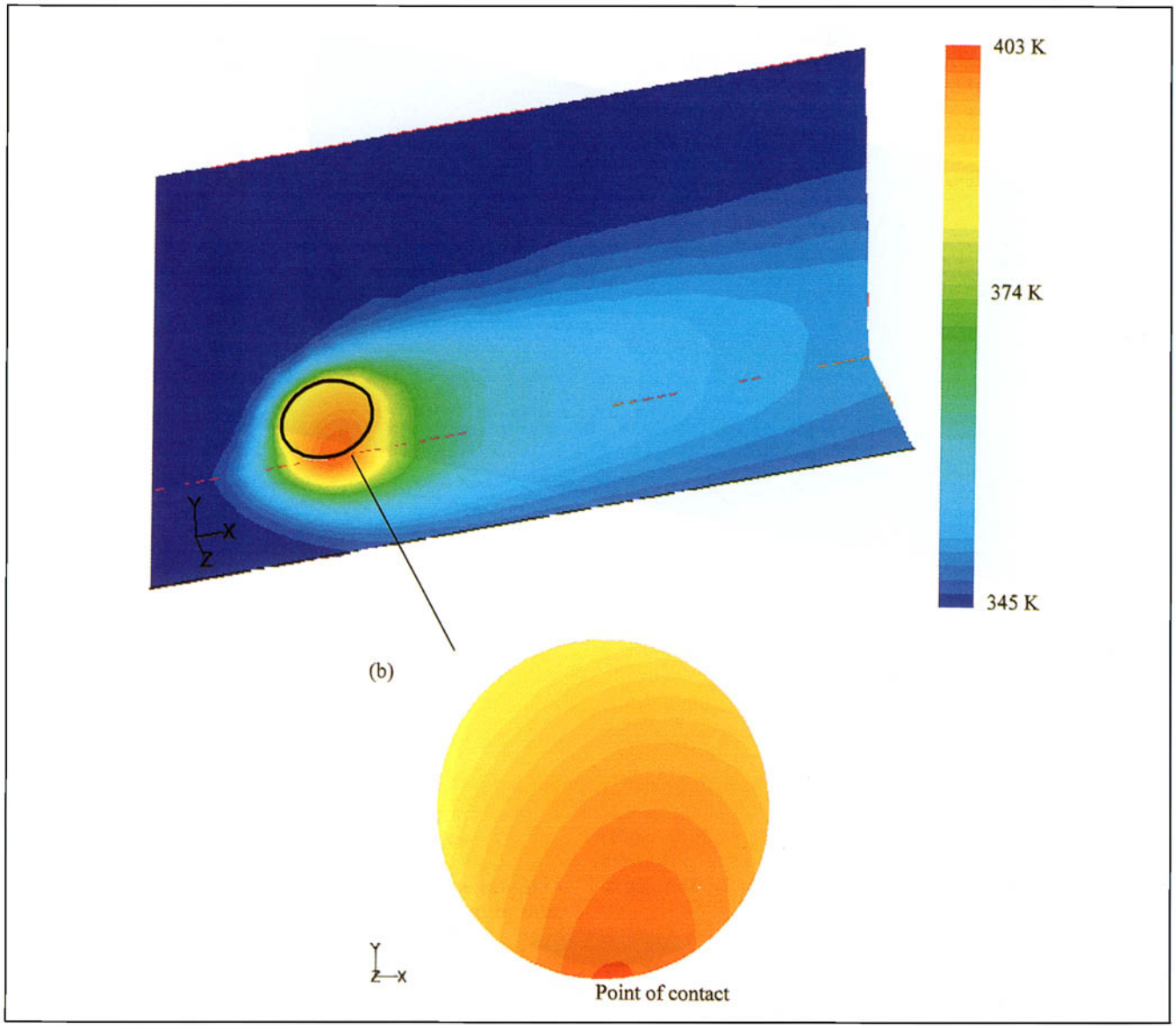

Figure 21. (a) Temperature contour map for a 20-μm particle touching an adiabatic wall (zero heat flux); (b) closeup of temperature profile.

ously, the cooler wall temperature certainly helps to cool the particle down, despite the relatively low local velocity due to proximity with the wall.

If on the other hand, since the reactor wall acts as an inert, adiabatic surface, we obtain the contour map shown in Figure 21. Once again, this is probably to be expected given that if no heat is removed by conduction with the inert surface, it must be evacuated by convection. We have already seen that this is not particularly effective in low-velocity situations. Although the local velocity along the particle surface is higher than that near the surface of the small particle in Figure 12, it is still not as high as in the case of the single, isolated particle. Thus, contact heating changes nothing, the wall slows the cooler fluid in the vicinity of the particle, and it obviously gets hotter than in the case of the single particle in the vicinity of the wall.

A comparison of the different temperature profiles in the system can be seen in Figure 22. In Figure 22a we can see the surface temperatures as a function of dimensionless axial position. The upper and lower portions of the two curves for the particle–wall cases represent the lower and upper surfaces of the particles, respectively (the simulation is not axisymmetric in this case, as it is for the single particle). Figure 22b shows the center-line temperatures. The contribution of convective heat removal can be seen by comparing the single particle and adiabatic wall cases. The major difference between these two geometries is in the local velocity at the particle surface, and in particular at the leading edge. The single-particle temperatures are lower, especially when compared to the lower surface of the adiabatic wall case, because the local velocity near the wall is almost zero.

Before finishing this last example, it is also interesting to

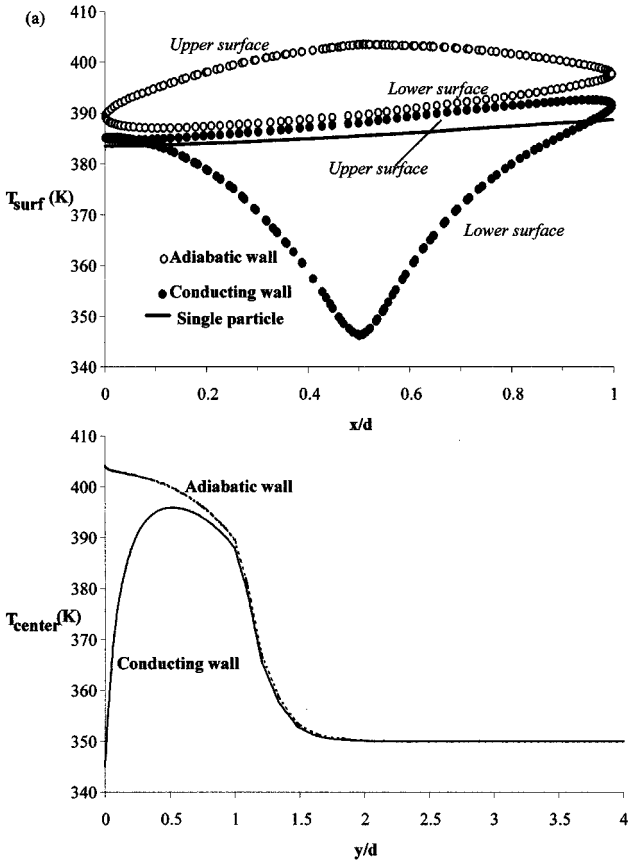

Figure 22. Interaction between small, hot particles and cold wall for both conducting wall at 345 K and for adiabatic wall.

(a) Temperature profiles at particle surface in the plane along the main direction of flow, and (b) temperature along the particle axis normal to the wall. Note that $Q = 4 \times 10^7$ kW/m^3 for small particle.

note that the temperature outside the particles, especially in the downstream direction, is relatively high. This means that highly active particles can cause significant temperature increases in their immediate vicinity. Therefore, although we have not tried to simulate this case, it would be interesting to look at just how close two particles have to be before they can cause each other to overheat. The results presented in Figures 5 and 6 suggest that shielding of one particle by another causes the local velocity of the downstream particle to drop, thereby leading to the creation of hot spots. However, this analysis did not take into consideration overheating by the neighboring particle. Nor did the analysis of the particle configuration in Figure 12. Here, the neighboring particles were essentially inert bodies. If two small particles are close enough, especially in a low-velocity zero, they might not even have to touch in order to provoke the formation of hot spots.

Conclusions

We have used CFD calculations to explore heat-transfer phenomena that occur during ethylene polymerization in a gas-phase reactor with conditions approaching those of a fluidized-bed reactor. This has turned out to be a very useful tool, allowing us to explore certain aspects of heat-transfer phenomena in a quantitative manner. Although the situations simulated here are admittedly very simplified with respect to what occurs in a real reactor, the quantitative results allow us to understand the relative importance of different mechanisms for heat removal from growing, highly active particles. The work presented here allows us to draw the following conclusions:

- We have validated the Ranz-Marshall correlation for single spheres. However, this correlation is only valid for highly diluted systems. If the particles are close enough together that the flow field around them is perturbed, the RM correlation will overpredict the value of *Nu* (and thus the heat-transfer coefficient) if one uses the relative particle–fluid velocity in the correlation. The implications of this should be obvious: any models employing this correlation to try and estimate how heat is removed from highly active particles will overpredict the importance of temperature profiles.
- If two particles of the same size and shape touch, a hot spot will form in between them.
- Particle shape (within reasonable limits, of course) does not have an overwhelming influence on convective heat-transfer coefficients. Particles in the shape of ellipsoids had surface-averaged values of *Nu* similar to those of single particles of the same relative size. Therefore the RM correlation, when valid, can be used for slightly elongated particles with no correction.
- Constant surface heat-flux calculations showed that under extremely ideal conditions, heat could be removed by convection from single particles in a free gas stream if the relative particle–gas velocity was high enough. However, if small, highly active particles were shielded from the gas flow without any contact, the reduced velocity in the area of the particle surface would lead to significant and rapid overheating.
- Contact between small, hot particles and larger, relatively cool ones helps to avoid overheating in the former, even when the local velocity at the particle surface is very low and convective heat transfer plays little to no role. The larger the contact point, the more exaggerated the effect of contact cooling. Similarly, contact with the reactor wall (or other cooling surfaces) has the same effect in a more pronounced way.
- Contact with an adiabatic surface does not improve heat transfer–in fact, it reduces the amount of heat that can be removed from a particle, because lower velocities in the neighborhood of a larger solid object lead to a reduction in convective heat transfer.
- Establishment of steady-state temperature profiles can be very rapid, with the temperature reaching 99% of its steady-state value in approximately 0.025 s. This means that overheating can occur very rapidly, or, conversely, that contact cooling can also be rapid.

The most significant conclusion is the fact that contact cooling can play such an important role in heat transfer. If one considers that FBRs are highly packed systems, with particles of many different sizes moving about very rapidly, it is not surprising that heat transfer is much more efficient than predicted with classic convection-only models during the first

few critical moments of polymerization on small, highly active particles. And, although this study did not look specifically at the case of stirred-bed reactors (SBR), these results also allow us to understand a bit more how heat transfer can occur there. From a ''heat transfer'' point of view, stirred-bed reactors differ from FBRs only in that the relative particle–gas velocities in the SBR are lower. Since it is common practice to put a small charge of large particles (or rock salt, etc.) in the reactor at the beginning of the polymerization to disperse the catalyst, it is reasonable to suppose that these same large particles absorb a good deal of heat from the smaller, more active ones, even in a batch reaction. In addition, a certain amount of heat might be removed through contact with the reactor wall. However, contact with the agitator in an SBR (especially in batch) might be more akin to the adiabatic wall situation if it is not maintained at a lower temperature. Thus a good deal of the deposits, and so forth, that one observes on the agitator and its axis might be due to localized overheating of the particles, as we saw in Figure 21.

Of course, it remains to be seen just how long contact times are and what more complex particle–particle interactions might produce in terms of heat transfer. Furthermore, it is entirely possible that it is necessary for particles to actually touch for overheating to take place (between two small particles), or for a cooling effect to take place (between large and small particles). It might in fact be sufficient for particles to pass close enough to one another for a short period of time in order for an interaction to take place. More advanced CFD simulations can be used in the next step to look at these possibilities. Nevertheless, the results are conclusive proof that heat-transfer modeling during the polymerization of ethylene must take more into account than simple convective heat transfer if we are to hope to obtain a good, quantitative description of the different phenomena occurring in the reactor.

Acknowledgments

Portions of this work have been funded by BRITE-EURAM project CATAPOL BE 3022.

Literature Cited

Brodkey, R. S., D. S. Kim, and W. Sidner, ''Fluid to Particle Heat Transfer in a Fluidized Bed and to Single Particles,'' *Chem. Eng. Proces.*, **18**, 157 (1984).

Ferrero, M. A., and M. G. Chiovetta, ''Catalyst Fragmentation During Propylene Polymerization: Part I. The Effects of Grain Size and Structure,'' *Poly. Eng. Sci.*, **27**, 1436 (1987a).

Ferrero, M. A., and M. G. Chiovetta, ''Catalyst Fragmentation During Propylene Polymerization: Part II. Microparticle Diffusion and Reaction Effects,'' *Poly. Eng. Sci.*, **27**, 1448 (1987b).

Ferrero, M. A., and M. G. Chiovetta, ''Catalyst Fragmentation During Propylene Polymerization: Part III. Bulk Polymerization Process Simulation,'' *Poly. Eng. Sci.*, **31**, 886 (1991a).

Ferrero, M. A., and M. G. Chiovetta, ''Catalyst Fragmentation During Propylene Polymerization: Part IV. Comparison Between Gas Phase and Bulk Polymerization Processes,'' *Poly. Eng. Sci.*, **31**, 904 (1991b).

Fluent 5, User's Guide, Fluent Inc., 10 Cavendish Court, Lebanon, NH 03766 (1998).

Floyd, S., K. Y. Choi, T. W. Taylor, and W. H. Ray, ''Polymerization of Olefins Through Heterogeneous Catalysis: III. Polymer Particle Modeling with an Analysis of Intraparticle Heat and Mass Transfer Effects,'' *J. Appl. Poly. Sci.*, **32**, 2935 (1986a).

Floyd, S., K. Y. Choi, T. W. Taylor, and W. H. Ray, ''Polymerization of Olefins Through Heterogeneous Catalysis. IV. Modeling of Heat and Mass Transfer Resistance in the Polymer Particle Boundary Layer,'' *J. Appl. Poly. Sci.*, **31**, 2231 (1986b).

Floyd, S., R. A. Hutchinson, and W. H. Ray, ''Polymerization of Olefins Through Heterogeneous Catalysis. V. Gas-Liquid Mass Transfer Limitations in Liquid Slurry Reactors,'' *J. Appl. Poly. Sci.*, **32**, 5451 (1986c).

Floyd, S., T. Heiskanen, T. W. Taylor, G. E. Mann, and W. H. Ray, ''Polymerization of Olefins Through Heterogeneous Catalysis. VI. Effect of Particle Heat and Mass Transfer on Polymerization Behavior and Polymer Properties,'' *J. Appl. Poly. Sci.*, **33**, 1021 (1987).

Hutchinson, R. A., and W. H. Ray, ''Polymerization of Olefins Through Heterogeneous Catalysis. IX. Experimental Study of Propylene Polymerization Over a High Activity $MgCl_2$-Supported Catalyst,'' *J. Appl. Poly. Sci.*, **43**, 1271 (1991).

Hutchinson, R. A., C. M. Chen, and W. H. Ray, ''Polymerization of Olefins Through Heterogeneous Catalysis: X. Modeling of Particle Growth and Morphology,'' *J. Appl. Poly. Sci.*, **44**, 1389 (1992).

Laurence, R. L., and M. G. Chiovetta, ''Heat and Mass Transfer During Olefin Polymerization from the Gas Phase,'' *Polymer Reaction Engineering: Influence of Reaction Engineering on Polymer Properties*, K. H. Reichert and W. Geisler, eds., Hanser, Munich (1983).

Martin, H., ''Low Peclet Number Particle-to-Fluid Heat and Mass Transfer in Packed Beds,'' *Chem. Eng. Sci.*, **33**, 913 (1979).

Martin, H., ''Heat Transfer Between Gas Fluidized Beds of Solid Particles and the Surfaces of Immersed Heat Exchanger Elements: I,'' *Chem. Eng. Process.*, **18**, 157 (1984).

Mathur, S. R., and J. Y. Murthy, ''A Pressure Based Method for Unstructured Meshes,'' *Numer. Heat Transfer*, **31**, 195 (1997).

McKenna, T. F., J. DuPuy, and R. Spitz, ''Modeling of Transfer Phenomena on Heterogeneous Ziegler Catalysts: Differences between Theory and Experiment, an Introduction,'' *J. Appl. Poly. Sci.*, **57**, 371 (1995a).

McKenna, T. F., H. Benamouama, and R. Spitz, ''Mass Transfer Resistance in Ziegler-Catalyzed Slurry Phase Polymerisation: A New Look at Reaction Modeling,'' *DECHEMA Monog.*, **131**, 223 (1995b).

McKenna, T. F., F. Barbotin, and R. Spitz, ''Modeling of Transfer Phenomena on Heterogeneous Ziegler Catalysts: Part 2. Experimental Investigation of Intraparticle Mass Transfer Resistance During the Polymerization of Ethylene in Slurry,'' *J. Appl. Poly. Sci.*, **62**, 1835 (1997a).

McKenna, T. F., J. DuPuy, and R. Spitz, ''Modeling of Transfer Phenomena on Heterogeneous Ziegler Catalysts: Part 3. Modeling of Intraparticle Mass Transfer Resistance,'' *J. Appl. Poly. Sci.*, **63**, 315 (1997b).

McKenna, T. F., D. Cokljat, and P. Wild, ''CFD Modeling of Heat Transfer During Gas Phase Olefin Polymerization,'' *Comput. Chem. Eng.*, **22**, S285 (1998).

McKenna, T. F., D. Cokljat, R. Spitz, and D. Schweich, ''Modeling of Heat and Mass Transfer During the Polymerization of Olefins on Heterogeneous Ziegler Catalysts,'' *Catal. Today*, **48**, 101 (1999).

Ranz, W. E., and W. R. Marshall, ''Evaporation from Drops,'' *Chem. Eng. Prog.*, **48**, 141 (1952).

Rowe, P. N., and K. T. Claxton, ''Heat and Mass Transfer from a Single Sphere to Fluid Flowing Through an Array,'' *Trans. Inst. Chem. Eng.*, **43**, T321 (1965).

Soares, J. B. P., and A. E. Hamielec, ''General Dynamic Mathematical Modeling of Heterogeneous Ziegler-Natta and Metallocene Catalyzed Copolymerisation with Multiple Site Types and Mass and Heat Transfer Resistance,'' *Poly. React. Eng.*, **3**, 261 (1995).

Taylor, T. W., K. Y. Choi, H. Yuan, and W. H. Ray, ''Physicochemical Kinetics of Liquid Phase Propylene Polymerization,'' *Transition Metal Catalyzed Polymerizations*, MMI Symp. Ser., **11**, Harwood Academic Pub., New York (1981).

Xie, T., K. B. McAuley, J. C. C. Hsu, and D. W. Bacon, ''Gas Phase Ethylene Polymerization: Production Processes, Polymer Properties and Reactor Modeling,'' *Ind. Eng. Chem. Res.*, **33**, 449 (1994).

Manuscript received Mar. 22, 1999, and revision received July 2, 1999.